Article

Hydrodynamic Limitations to Mangrove Seedling Retention in Subtropical Estuaries

Kelly M. Kibler [1,*], Christian Pilato [2], Linda J. Walters [3], Melinda Donnelly [3] and Jyotismita Taye [4]

[1] Department of Civil, Environmental & Construction Engineering and National Center for Integrated Coastal Research, University of Central Florida, 4000 Central Florida Blvd., Orlando, FL 32816, USA

[2] Department of Biology, University of Central Florida, 4000 Central Florida Blvd., Orlando, FL 32816, USA; pilato.christian1@gmail.com

[3] Department of Biology and National Center for Integrated Coastal Research, University of Central Florida, 4000 Central Florida Blvd., Orlando, FL 32816, USA; linda.walters@ucf.edu (L.J.W.); melinda.donnelly@ucf.edu (M.D.)

[4] Department of Civil, Environmental & Construction Engineering, University of Central Florida, 4000 Central Florida Blvd., Orlando, FL 32816, USA; jyotismita.taye@ucf.edu

* Correspondence: kelly.kibler@ucf.edu; Tel.: +1-407-823-4150

Abstract: Mangrove-forest sustainability hinges upon propagule recruitment and seedling retention. This study evaluates biophysical limitations to mangrove-seedling persistence by measuring anchoring force of two mangrove species (*Rhizophora mangle* L. and *Avicennia germinans* (L.) L.). Anchoring force was measured in 362 seedlings via lateral pull tests administered in mangrove forests of two subtropical estuaries and in laboratory-based experiments. Removal mechanism varied with seedling age: newly established seedlings failed due to root pull-out while seedlings older than 3 months failed by root breakage. The anchoring force of *R. mangle* seedlings was consistently and significantly greater than *A. germinans* ($p = 0.002$); however, force to remove *A. germinans* seedlings increased with growth at a faster rate ($p < 0.001$; *A. germinans*: 0.20–0.23 N/g biomass; *R. mangle*: 0.04–0.07 N/g biomass). Increasing density of surrounding vegetation had a positive effect ($p = 0.04$) on anchoring force of both species. Critical velocities at which seedlings become susceptible to instantaneous uprooting estimated from anchoring forces measured in the field were 1.20 m/s and 1.50 m/s, respectively, for *R. mangle* and *A. germinans*. As estimated critical velocities exceed typical flow magnitudes observed in field sites, removal of established seedlings likely occurs following erosion of sediments from the seedling base.

Keywords: coastal sustainability; mangrove recruitment; living shoreline; restoration; hydrodynamics; bank erosion; wetlands; natural infrastructure

1. Introduction

Mangrove vegetation provides a vast array of ecosystem services to coastal systems, including the regulation of biogeochemical cycling, notably carbon sequestration, provisioning of raw materials, and habitat for a variety of ecologically and economically important fauna [1–4]. Mangrove forests are increasingly recognized for their ecosystem engineering potential to dissipate hydrodynamic forces, store carbon and promote sediment accretion in low-lying areas [5–8]. As coastal communities in tropical and subtropical regions, including developing economies and small-island states, have great need to adapt to climate-change-related sea level transgression and more frequent storms, there is keen stakeholder interest in utilizing mangrove as an ecosystem engineer to promote coastal stability [1,8]. Despite their intrinsic ecological and economic importance, a substantial decline in global mangrove cover has been observed, with an overall ~35% reduction in habitat size since the 1980s [9–11]. This decline has been attributed to a variety of anthropogenic stressors, including coastal development, aquaculture expansion, and

hydrological change [2,11–13]. Outcomes in restoring degraded habitats to self-sustaining mangrove forests have been variable, with mismatches in mangrove habitat preferences and site hydrodynamics often cited as a root cause of planting failures [14].

Mangroves inhabit mechanically challenging environments characterized by complex biophysical feedbacks [15,16]. In addition to eco-physiological stressors of salinity, temperature [17] and water level fluctuation [16], fringe forests on channel margins and lagoon shorelines are exposed to varied hydrodynamic forcings that create a dynamic morphological environment. For instance, hydrodynamic forces may range from tidal and riverine currents to tropical-storm-force winds and waves [1,18]. Mature mangrove communities routinely withstand and dissipate local hydrodynamic energy (e.g., [1,7,19]), yet hydrodynamic limitations to the development of mature mangrove forests on open-water fringes have been detected [20]. Similar hydrodynamic habitat thresholds for mangroves have been estimated in the subtropical Atlantic (80th percentile wave height of 80 mm, [20]) and tropical Western Indian Ocean (mean wave height of 61 mm, [21]). Understanding the hydrodynamic niche of mature mangroves is incredibly useful in restoration planning and the design of robust natural infrastructure [14,20,22]. However, little information is available to characterize mangrove seedling interactions with hydrodynamic and sediment transport mechanisms during the critical early-life history stages that are vital for habitat succession and long-term forest structure [23].

Recruitment occurs when mangrove propagules end their free-floating dispersal phase by rooting into the substrate, becoming seedlings with single, flexible stems and few leaves [24]. While the early establishment phase is characterized by rapid root and stem growth [25], seedlings are particularly vulnerable to physical stressors, including inundation and dislodgement by hydrodynamic forces [17,26]. Dislodgement of vegetation by hydrodynamic force is classified according to the specific geomorphic mechanism of dislodgement [27]: Type I removal occurs instantaneously when the hydrodynamic drag force exceeds the plant anchoring force. By contrast, Type II removal occurs in conjunction with erosion of sediment from the base of the plant, which reduces anchoring force over time. Type II removal is further classified to distinguish between local erosion around individual plants (Type IIa) as opposed to larger scale erosion, for instance, degradation of entire shorelines or river bars (Type IIb) [28]. As erosion around plant roots takes place over time, during which the plant is also increasing its anchoring force through growth, the dynamic interplay of plant growth vs. net erosion rate will ultimately determine resistance of the plant to Type II removal [29].

Hydrodynamic forces (e.g., waves and currents) guide mangrove colonization and constrain seedling persistence in dynamic intertidal environments [15,30]. However, specific hydrodynamic limitations and mechanisms of seedling removal have not been well-characterized in the field [15,23,31]. This study characterizes seedling resistance to removal through Type I mechanisms for two mangrove species, *Avicennia germinans* (L.) L. and *Rhizophora mangle* L.. Both species are representatives from circumtropical genera and showcase unique life-history strategies. *R. mangle* propagules, and subsequently seedlings, are larger than *A. germinans* and have thicker hypocotyl and differing leaf morphologies, particularly in early-life stages [32]. Propagules of these two species also display differing recruitment strategies. *A. germinans*, and other *Avicennia* spp., are recognized as colonizers within tropical wetland systems [23,33,34]. *A. germinans* exhibit traits typical of pioneer species such as rapid early-growth rates and greater resource partitioning to leaf area [35]. Alternatively, *R. mangle* is described as an opportunistic gap species [36]. Although both species are codominant in low- to mid-tide levels across their native ranges, differences in recruitment strategies may affect susceptibility to hydrodynamic dislodgement and thus influence colonization success. We hypothesize that the differing morphologies and recruitment strategies will alter interactions with the hydrodynamic environment to determine species-specific thresholds. The goal of the study is to quantify these species-specific hydrodynamic thresholds through early growth stages and to elucidate mechanisms of seedling dislodgement to improve understanding of mangrove retention

in areas of hydrodynamic stress, such as restored fringe forests and active shorelines. We address research questions of whether and how hydrodynamic thresholds influence mangrove seedling retention across the species of study, time since establishment and in response to environmental variables such as sediment characteristics and surrounding vegetation.

2. Materials and Methods

Anchoring force of mangrove seedlings was measured in the field (in situ) and laboratory using lateral pull tests. Field measurements were conducted in two mangrove forests located in coastal Florida, USA. Laboratory experiments were conducted in a controlled environment at the University of Central Florida. For laboratory experiments, mangrove seedlings were grown from propagules collected from field sites in a hoop-style greenhouse with plastic roofing and screened sides.

2.1. Site Description

In-situ lateral pull tests were undertaken in two locations: in Tampa Bay at De Soto National Memorial (DSNM) (27.523889° N, 82.644444° W) and in Mosquito Lagoon at Canaveral National Seashore (CANA) (28.7675° N, 80.776944° W). DSNM (Figure 1a) is located on the Gulf coast of Florida where the Manatee River enters Tampa Bay [37]. CANA (Figure 1b) is located along the Atlantic coast of Florida within Mosquito Lagoon, a shallow, microtidal estuary that is the northernmost waterbody of the Indian River Lagoon system [38]. The climate in both locations is humid subtropical, with mean annual precipitation around 1000 mm. Water temperatures in CANA range from 4–33 °C, and salinities range from 22.6–45.2 ppt [39]. In DSNM, salinities range from 1.0 to 33.7 ppt and water temperatures range between 11.3–32.2 °C [40]. In both sites, mangrove forest is the dominant wetland vegetation type within intertidal ecotones, and *A. germinans* and *R. mangle* are the most common mangrove species. *Laguncularia racemose* (L.) Gaertn is also found in the study area, typically landward of *A. germinans* and *R. mangle*. As *L. racemose* inhabit areas that are comparatively less geomorphologically active [34], this species was not tested. Active shoreline restoration is ongoing in both locations, incorporating living shoreline techniques of emergent halophytic grass and mangrove plantings to combat widespread shoreline erosion [17]. To test the Type I removal thresholds of mangrove seedlings, study sites were chosen from within mature reference-condition mangrove forests (2 forest patches in CANA, 3 forest patches in DSNM) where evidence of erosion (e.g., scarping and slumping, exposed roots of vegetation) was not observed.

Figure 1. Field site locations within (**a**) De Soto National Memorial and (**b**) Canaveral National Seashore.

2.2. Lateral Pull Test

Lateral pull tests (Figure 2) were conducted to measure the resistance of mangrove seedlings to instantaneous uprooting given intact (non-eroded) surrounding sediments. The horizontal component of force recorded at the moment of seedling dislodgment estimated the seedling's anchoring force, and, therefore, resistance to hydrodynamic drag. Pull-test methods were adapted from [28], and were applied similarly in both laboratory and field experiments.
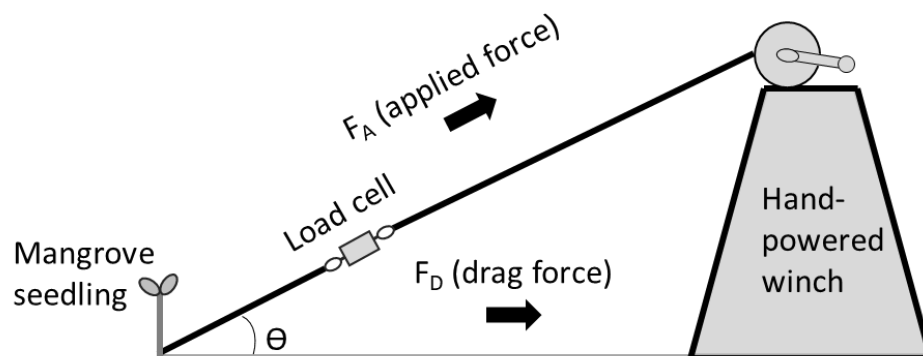
Figure 2. Lateral pull test design.

Seedlings were attached to an anchored hand winch using a 4.8 mm nylon rope attached at the seedling base above the sediment line (Figure 2). The rope was attached to a 3.2 mm steel wire connected to a load cell (Omega, max force = 111 N; error = 0.25%) and the hand winch. The force exerted on each seedling when tension was applied by the hand winch was continuously measured at 2 Hz by the load cell and logged using a Campbell Scientific CR850 data logger. The horizontal resistance force (F_R), or equivalently, the horizontal drag force, to removal, (F_D) of each mangrove seedling was calculated by Equation (1):

$$F_R = F_A \cdot \cos \theta, \tag{1}$$

where F_A is applied force measured at time of uprooting (N, Newtons) and θ is the angle between F_A and horizontal, which was measured in the field. The pulling angle was restricted to well below 35° to ensure that the horizontal component was the dominant component of applied force.

2.2.1. Field Data Collection

For field trials, mangroves seedlings (all single-stemmed, with flexible and non-woody stem, few leaves, and no aerial roots [24], Figure 3) were haphazardly selected from each forest patch. Approximately 45 each of *R. mangle* and *A. germinans* seedlings were selected from each site for a total of 182 seedlings (87 *A. germinans* and 95 *R. mangle*). Field trials were run between May and August. Tested seedlings had recruited from the prior year's propagule stock, released approximately 7–11 months prior to testing. Field pull tests were conducted when water levels were sufficient to saturate sediments surrounding each seedling to the sediment surface. Groundcover surrounding each seedling, including mature mangrove root structure, was characterized prior to pull-tests using the point intercept method [41] within a 0.25 m² quadrat centered on the seedling. All species of vegetation within the quadrat were counted and identified to species level. Canopy cover was quantified using a GRS densitometer (Geographic Resource Solutions) held directly above each seedling and at four separate right angles from the seedling.

Figure 3. *Avicennia germinans* (L.) L. (**left**) and *Rhizophora mangle* L. (**right**) mangrove seedlings sampled in the field.

2.2.2. Laboratory Data Collection

To understand how anchoring of *A. germinans* and *R. mangle* seedlings varies as a function of early seedling development and sediment characteristics, laboratory testing was undertaken in a controlled greenhouse environment. Propagules of both species were haphazardly collected from trees in CANA and planted in 1-gallon pots for a total of *n* = 180 sown seedlings (90 *A. germinans*, 90 *R. mangle* seedlings). Propagules were not sorted by size before planting and thus reflect the natural size-class variability of the field site. Propagules were randomly planted in one of two sediment treatments designed to represent the range of particle distributions observed on eroded shorelines where mangrove restoration often takes place [42,43]. Sediment treatments were comprised of sand and gravel-sized oyster shells that were either "whole" shells or "crushed" by mechanical weathering. Both sediment treatments contained 50% commercial sand by volume (no organics) and 50% oyster shell. However, the size of larger particles (oyster shell) varied between the two treatments (crushed: mean shell size = 1.5 ± 0.25 cm, whole: mean shell size: 5.9 ± 0.3 cm).

Locations of pots were randomized within the growing space and filled flush with sediment before planting. In addition, 1-gallon pots were contained in larger 15-L plastic tubs to maintain constant water levels. Each tub was watered to a 23 cm depth weekly with fresh water. After 1, 3, and 4 months, a total of 60 mangroves (15 of each species from each sediment treatment) were randomly selected and uprooted in lateral pull tests (Figure 4).

Figure 4. *Avicennia germinans* (L.) L. (**top**) and *Rhizophora mangle* L. (**bottom**) mangrove seedlings sampled in the lab one month after establishment.

2.3. Seedling and Sediment Characterization

Seedling morphometrics were recorded for all seedlings uprooted in the field or laboratory. Seedling height was measured from the sediment base to the tip of the tallest leaf, basal diameter was measured at the lowest point of the mangrove hypocotyl directly above the substrate surface, and the total number of leaves were counted. Seedling frontal area was characterized using a digital camera with a white background with vertical and horizontal scale bars, as described in Lightbody and Nepf [44]. Images were hand digitized and processed through ImageJ image-processing and analysis software (ver. 1.46r). Wet and dry above- and below-ground biomass were measured after seedlings were removed from the sediment. Detached root mass was retrieved from sediment after each pull test. Sediments were extracted from each seedling location and detached roots were visually identified and added to below-ground biomass measurements.

Five bulk sediment samples were taken from each forest patch to a depth of 10 cm using an acrylic core (diameter: 10 cm). Core samples were dried at 110 °C and aggregated by patch (mean ± S.E. dry mass of aggregated sample = 637.36 ± 138.52 g), then analyzed for particle size distribution and organic-matter (OM) content. OM content was evaluated as loss upon ignition at 550 °C in a muffle furnace for 16 h, using 20 g subsamples. Grain size distributions were characterized using dry and wet sieve analyses using sieve sizes ranging from 76.200 mm to 0.067 mm [45].

2.4. Data Analysis

Generalized linear models (GLM) were used to model the influence of environmental and morphometric variables on the force required to uproot mangrove seedlings, with alternative models constructed and compared via corrected Akaike Information Criteria (AICc) weights from the R package "bbmle" [46]. The response variable for all models was F_R, the horizontal force to removal (Equation (1)). Predictor variables for field tests included species, above/below-ground biomass, seedling height, leaf number, base diameter, seedling frontal area, sediment grain size, percent organic matter, percent ground-cover of surrounding vegetation, and percent canopy cover. Anchoring force measured in laboratory experiments was tested against predictor variables of species, age, above/below-ground biomass, seedling height, seedling frontal area, and sediment treatment.

While creating the candidate models for laboratory and in-field pull tests, alternative measures of plant size were tested individually (e.g., height, basal diameter, frontal area, leaf number). As these metrics were collinear, only one plant size variable was used in any candidate model. The data were effectively modeled using linear regression after natural log transformation of the response variable. All statistical analyses were performed with R 3.5.1 software [47]. All graphs were constructed using the "ggplot2" package in R [48].

3. Results

3.1. Field Pull Tests: Anchoring Force in Mangrove Forest

Seedling removal in the field occurred through two distinct mechanisms. Uprooting occurred when the roots failed (broke) or were pulled intact from surrounding sediments. Root breakage was the dominant failure mechanism observed in situ as few seedlings (16.5%) were removed with no root breakage. Mechanism of removal did not vary systematically by location or species. Location did not have a significant effect on horizontal force to removal (GLM: t = −0.436, *p* = 0.664); therefore, data from all locations were pooled for analysis. Magnitude of removal force in the field was strongly related to mangrove size and varied between species (Figure 5, Table 1). Force to remove *R. mangle* seedlings in the field (range: 8.1–114.3 N; mean ± S.E.: 47.3 ± 2.6 N) was significantly greater than magnitude of force to remove *A. germinans* (range: 4.0–47.3 N; mean ± S.E.: 18.8 ± 0.9 N) (GLM: t = 3.189, *p* = 0.002).
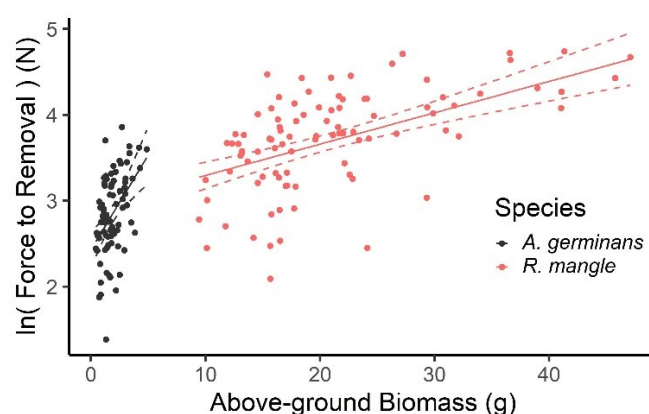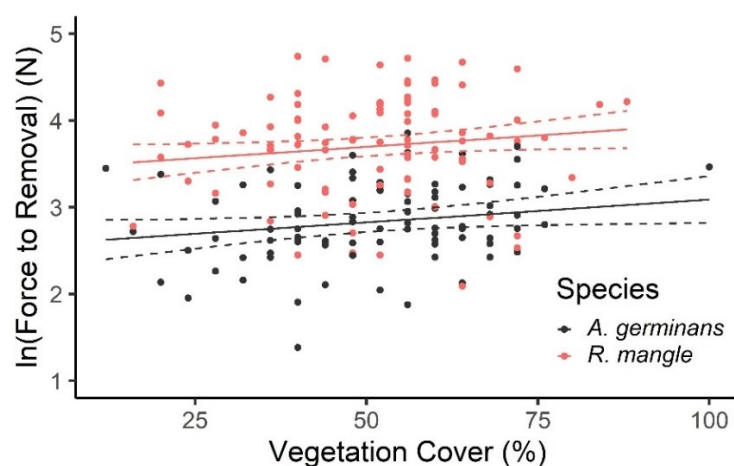

Figure 5. Linear regression models with 95% confidence intervals for anchoring force of *Rhizophora mangle* L. and *Avicennia germinans* (L.) L. measured in field pull tests as a function of above-ground biomass.

Table 1. Parameter estimates for best linear models (Tables A1 and A2) of field ($R^2 = 0.5645$) and laboratory ($R^2 = 0.8461$) pull tests. Coefficients are based on *Avicennia germinans* (L.) L. set as the reference level for field tests and 1 month *A. germinans* grown in the whole-shell sediment treatment as the reference level for laboratory tests.

		Estimates	Std. Error	t Value	Pr(>|t|)
Field tests:	Intercept	2.180934	0.15793	13.809	<0.001
	Above-Ground Biomass	0.22507	0.05033	4.472	<0.001
	Rhizophora mangle L.	0.52852	0.16573	3.189	0.0017
	Percent Vegetation	0.00468	0.00224	2.092	0.0379
	Above-Ground Biomass: *R. mangle* L.	−0.18942	0.05067	−3.739	<0.001
Lab tests:	Intercept	1.74262	0.07502	24.346	<0.001
	Below-Ground Biomass	0.19579	0.03580	5.352	<0.001
	Rhizophora mangle L.	0.93614	0.14639	6.388	<0.001
	Crushed shell	0.28001	0.05431	2.178	0.0309
	3 months	0.75687	0.07717	8.796	<0.001
	4 months	1.01866	0.07727	10.993	<0.001
	Below-Ground Biomass: *R. mangle* L.	−0.13226	0.03578	−3.585	<0.001
	Crushed shell: 3 months	−0.16509	0.12749	−1.295	0.197
	Crushed shell: 4 months	−0.35429	0.13143	−2.696	0.008

Seedlings of *R. mangle* were larger than *A. germinans* seedlings according to all size metrics (Table 2). The hypocotyl of *R. mangle* seedlings were thicker than those of *A. germinans* seedlings (e.g., Figures 3 and 4) and the mean (±S.E.) above-ground biomass of *R. mangle* seedlings (21.16 ± 0.86 g) was an order of magnitude larger than that of *A. germinans* seedlings (1.83 ± 0.11 g). The greater above-ground biomass contributed to *R. mangle*'s considerably greater frontal area (53.47 ± 4.07 cm²) when compared to *A. germinans* seedlings (10.89 ± 0.62 cm²). Model selection indicated that above-ground biomass was the best of the co-linear plant size metrics to predict horizontal force to removal in the field and this variable was used for all later alternative field models. While significantly greater force was required to remove *R. mangle* seedlings in general, a significant interaction between above-ground biomass and mangrove species was also observed. Force to remove *A. germinans* seedlings increased at a faster rate in response to biomass increases (0.23 N per 1 g increase in biomass, 95% CI: 0.13, 0.32) as compared to *R. mangle* seedlings (increase of 0.04 N per 1 g increase in biomass, 95% CI: 0.03, 0.05, GLM: $t = -3.739$, $p < 0.001$, Figure 5).

Table 2. Mean summary statistics (±S.E.) for seedlings tested in field lateral pull tests.

Species	N	Park	Above-Ground Biomass (g)	Below-Ground Biomass (g)	Height (cm)	Leaf Number	Basal Diameter (cm)
Rhizophora mangle L.	95	CANA	24.9 ± 1.4	6.4 ± 0.4	42.8 ± 1.3	7.5 ± 0.5	1.2 ± 0.0
		DSNM	17.7 ± 0.8	6.6 ± 0.4	35.5 ± 0.9	5.1 ± 0.3	1.2 ± 0.0
Avicennia germinans (L.) L.	87	CANA	2.1 ± 0.1	0.6 ± 0.0	21.8 ± 0.6	4.7 ± 0.2	0.4 ± 0.0
		DSNM	1.4 ± 0.2	0.7 ± 0.1	19.7 ± 0.9	4.5 ± 0.3	0.3 ± 0.0

The canopy in all forest patches was dominated by mature *R. mangle* and *A. germinans* trees and vegetated groundcover consisted almost entirely of *A. germinans* pneumatophores. Established seedlings were found growing in and among dense assemblages of aerial roots. Force to removal increased with groundcover density (GLM: $t = 2.092$, $p = 0.04$); a one percent increase in groundcover density led to a 0.005 N (95% CI: 0.0003, 0.009 N) increase in force to removal. This trend was consistently positive for *A. germinans* while the highest force to removal for *R. mangle* was observed in areas with intermediate vegetation cover (Figure 6). Canopy closure was not found to have a significant effect on the horizontal force to removal for either species. While sediment-grain size distributions and

organic-matter content varied somewhat across field sites, median sediment grain sizes were similar and no differences in force to removal related to sediment characteristics were detected (Table 3, Figure 7).

Table 3. Summary sediment parameters by site/treatment.

Site/Treatment	D50 (mm)	D16 (mm)	D84 (mm)	Organic Matter (%)
Field testing				
CANA 1	0.18	0.04	0.50	29.7
CANA 2	0.21	0.08	0.49	16.0
De Soto 1	0.32	0.16	1.88	28.5
De Soto 2	0.46	0.06	6.21	56.4
De Soto 3	0.22	0.15	0.42	10.4
Laboratory testing				
Crushed shell-sand	0.38	0.19	2.28	—
Whole shell-sand	0.44	0.21	19.3	—

Figure 6. Linear regression model with 95% confidence intervals for anchoring force of *Rhizophora mangle* L. and *Avicennia germinans* (L.) L. recorded in field pull tests as a function of groundcover density (%) in surrounding 0.25 m².
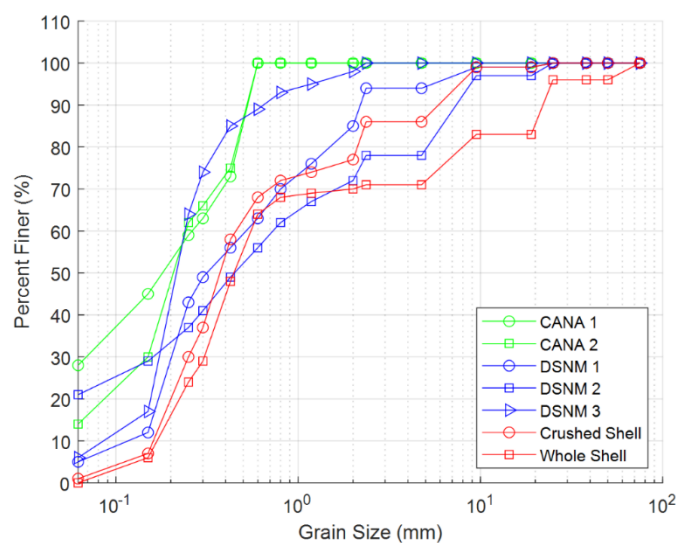

Figure 7. Grain size distributions of field sediments by site and laboratory sediment treatments.

3.2. Laboratory Pull Tests: Anchoring Force Across Seedling Age

As in the field, biometrics varied according to species (Table 4) and force to remove seedlings in laboratory testing was strongly related to plant size (Table 1, Figure 8). In the early post-germination stages tested in the laboratory, below-ground biomass was the best plant size metric to predict horizontal force to removal for both mangrove species at all ages. Below-ground biomass was, therefore, selected for all alternative laboratory models. Significantly more force was required to remove seedlings as biomass increased (GLM: t = 5.352, $p < 0.001$). For instance, a 1 g increase in biomass led to a mean 0.20 N (95% CI: 0.13, 0.27) increase in horizontal force to removal for *A. germinans* seedlings. Analogous to field observations, the force to remove *A. germinans* seedlings increased at a faster rate as biomass increased. The increase in the force to remove *R. mangle* seedlings per gram of increased biomass was comparatively low (0.07 N, 95% CI: 0.06, 0.08). For all age classes, the mean force required to remove *R. mangle* seedlings was significantly greater (GLM: t = 6.388, $p < 0.001$) than that required to remove *A. germinans* seedlings (Figure 8, Table 4).

Table 4. Mean summary statistics (±S.E.) for seedlings tested in laboratory pull tests.

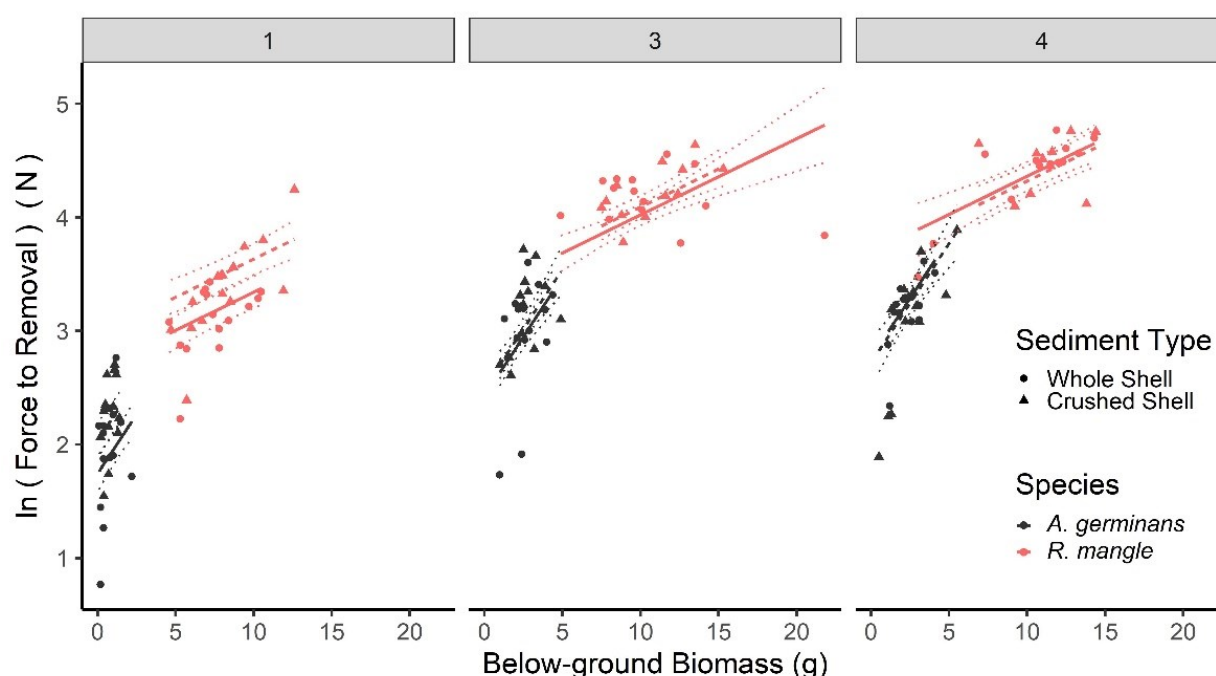| Species	Age (months)	N	Above-Ground Biomass (g)	Below-Ground Biomass (g)	Height (cm)	Force to Removal (N)
Rhizophora mangle L.	1	30	16.0 ± 0.7	7.8 ± 0.4	25.2 ± 0.9	27.2 ± 2.0
	3	30	19.3 ± 0.7	10.7 ± 0.7	31.8 ± 0.9	68.1 ± 3.1
	4	30	18.3 ± 1.2	10.6 ± 0.6	31.2 ± 1.4	86.7 ± 4.7
Avicennia germinans (L.) L.	1	30	2.7 ± 0.2	0.8 ± 0.1	9.5 ± 0.5	9.1 ± 0.6
	3	30	2.4 ± 0.2	2.6 ± 0.2	15.2 ± 0.6	22.7 ± 1.5
	4	30	2.6 ± 0.3	2.4 ± 0.2	15.2 ± 0.8	25.0 ± 1.8

Figure 8. Linear regression model with 95% confidence intervals of 1-, 3- and 4-month old *Avicennia germinans* (L.) L. and *Rhizophora mangle* L. anchoring force measured in laboratory pull tests as a function of below-ground biomass.

The dominant seedling failure mechanism observed in laboratory testing changed after one month. Root breakage failure was not observed in removal of any 1-month

seedlings while only 3% of seedlings in the 3- and 4-month age classes were removed with intact roots. Seedling age also had a significant effect on force to removal of both species (3 month GLM: t = 8.796, *p* < 0.001; 4 month GLM: t = 10.993, *p* < 0.001).

Though the distributions of laboratory sediment treatments were similar up to the 1 mm size class (Figure 7), the differences in coarse fractions had a significant effect on force to remove 1-month old seedlings. At 1 month, the crushed-shell sediment treatment had a significant positive effect (GLM: t = 2.178, *p* = 0.03); the mean force to remove seedlings grown in the finer sediment treatment was 37% greater across both species as compared to the whole-shell treatment. Despite this initial positive relationship, the effect of sediment size on force to removal changed as seedlings aged and no effect of sediment size was detected in 3- and 4-month-old seedlings.

3.3. Minimum Flows Required for Type I Dislodgement of Mangrove Seedlings

The magnitudes of anchoring force measured in this study can be recast as flow thresholds above which mangrove seedlings may become susceptible to instantaneous (Type I) uprooting. Critical velocities can be estimated by equating the measured anchoring force to a drag force at removal, $F_D = \frac{1}{2} \rho C_D A U^2$, where ρ is the density of seawater (1030 kg/m³), C_D is the drag coefficient, A is the frontal area of the seedling, and U is the mean horizontal velocity [28]. Using Monte Carlo simulations (N = 1000) where parameters are randomly selected from their respective distributions (e.g., species-level truncated normal distributions of measured removal force and frontal area, area reduction coefficient to account for seedling pronation (range: 0.4–1.0; mean = 0.7; S.D. = 0.08, [28]), drag coefficients (range: 0.02–10; mean = 1; S.D. = 0.8, [19,30,49,50])), the flow speed required for instantaneous removal can be probabilistically estimated. Based on field data, established *A. germinans* seedlings may become susceptible to spontaneous uprooting when velocities exceed 1.50 m/s and *R. mangle* seedlings are estimated to become susceptible when velocities exceed 1.20 m/s.

4. Discussion

4.1. Seedling Size and Age Influence Anchoring Force and Mechanism of Removal

A positive relationship between mangrove seedling size (biomass) and force to removal was observed across both mangrove species tested (0.20–0.23 N/g in *A. germinans* and 0.04–0.07 N/g in *R. mangle*), and trends were similar in field and laboratory testing. The relationship of plant size to anchorage force has been reported consistently in the literature, for instance, from winching experiments of terrestrial species [51–55]. Similarly, influence of seedling size to resistance force is reported in studies that applied comparable pull-test methodologies to quantify resistance of floodplain woody vegetation (1–2-year-old cottonwood *Populus deltoides*, [56]; 1–5-year-old *Populus* spp. and *Tamarix* spp., [28]; 2–6-year-old *Alnus incana, Populus nigra, Salix elaeaganos*, [57]; 4-year-old *Salix alba*, [58]). The same conclusions are reached for submerged aquatic vegetation [59], newly established mangrove seedlings (*Avicienna alba*, [23]) and 1–3-year-old red mangrove trees (*R. mangle*, [24]). In this study, multiple alternative measures of plant size were tested and compared to understand the morphometric variables most strongly related to seedling anchoring. The co-linear metrics of plant size (e.g., height, frontal area, weight/mass, basal diameter) often related to anchoring force are indicators correlated to the causal mechanisms of resistance, which are a combination of the rooting size (length, depth, mass), architecture and tensile strength. For example, Bankhead et al. [56] observed that root size and strength were related to the failure mechanism and resistance force in mature invasive reed canarygrass (*Phalaris arundinacea*) and common reed (*Phragmites australis*). In contrast, total root length and distribution of primary and secondary root structures were found to be influential to anchoring force of 2–6-day-old oat (*Avena sativa*) and alfalfa (*Medicago sativa*) seedlings [60]. Similarly, Balke et al. [23] observed that the force and hydrodynamic shear stress needed to remove newly established (<2 weeks) mangrove seedings was related to

the maximum root length. Though not formally quantified in this study, the rooting architecture of *A. germinans* and *R. mangle* differ (Figure 4), which may contribute to the observed species-level differences in anchoring force.

As seedling age and size (e.g., root mass) are co-linear, it is not surprising that older seedlings (>3 months) were also associated with stronger anchoring forces. However, this study identifies a threshold in mangrove seedling development that relates to anchoring and vulnerability to removal during early-life-history stages. Two prior studies have measured mangrove anchoring force, respectively, in newly germinated seedlings (*Avicienna alba*, 2–13 days after planting) and established transitional to sapling mangrove (*R. mangle*, 1–3 years after natural recruitment). The magnitudes of force to remove *R. mangle* seedlings grown in the greenhouse or in forests observed in this study are within the lower range of forces reported for older plants (1–3 years) of the same species growing naturally (2–481 N, [24]). All *A. alba* seedlings tested by Balke et al. [23] were removed with forces of less than 6 N, which is less than the mean force that was required to remove the seedlings with lowest mean anchoring force and belowground biomass observed in this study: the 1-month seedlings (*R. mangle* mean 27.2 N and *A. germinans* mean 9.1 N). However, between 1 and 3 months, force required for removal of both the species observed in this study increased significantly and the dominant mechanism of removal shifted from pulling out of intact roots to root breakage. Root breakage was also the dominant mechanism observed in older seedlings growing in mangrove forest. The force threshold and mechanism change from 1-month to 3-month-and-older seedlings suggests that small root size and limited structure are the main source of vulnerability for newly established seedlings. As the rooting architecture becomes more extensive and complex, anchoring by root–soil interaction eventually surpasses root strength (observed here in laboratory testing by 12 weeks) and tensile strength of roots becomes the limiting factor to anchoring more established seedlings, as greater force is required to dislodge the root mass intact as compared to break the roots.

The impact of rooting mass to anchoring force is also evident in the larger forces required to dislodge 3–4-month seedlings grown in the greenhouse as compared to seedlings in mangrove forest patches. This finding is surprising, as seedlings tested in the field were likely to have been established for more than 4 months and anchoring force in the field was found to be enhanced by physical interaction with surrounding vegetation. However, mean root mass measured in the forest seedlings was 29% lower for *R. mangle* and 65% lower for *A. germinans* than in 3- and 4-month greenhouse seedlings. Seedlings growing in the shaded forest environment likely focused growth to above-ground biomass [61] while the larger below-ground biomass stock recorded in greenhouse seedlings reflects that seedlings grown in isolation, in fresh water, and facing no competition for light or nutrients were able to store greater root mass [35,62], which led to comparatively larger force to removal.

4.2. Influence of Sediment and Surrounding Vegetation to Seedling Anchoring

In this study, sediment texture was not found to relate strongly to the anchoring force of mangrove seedlings older than 3 months (including all seedlings tested in the field and 3–4-month-old seedlings tested in the laboratory), but was found to be influential during very early seedling establishment. Seedlings of both species tested at 1 month in the laboratory required significantly greater force to remove when rooted in a finer sediment distribution, an effect that was consistent across seedling biomass. The divergent effect of sediment texture with seedling age observed in this study may indicate that sediment characteristics most noticeably affect anchoring in the initial stages of seedling development, which may explain some discrepancies within the prior literature reporting on this question.

For example, several prior studies report that plants rooted in finer sediments have greater resistance to uprooting [57,60,63]. This effect has been attributed to different rooting architectures developing in response to sediment size, for example, the round form of

roots that developed in sand versus irregular form of roots in gravel [63]. The cohesive strength of sediment was also found to be influential to root failure. For instance, Schutten et al. [59] report increased anchorage strength for aquatic plants growing in firmer (1.5 kPa), as opposed to softer, sediments (0.1 kPa). However, Boizard and Mitchell [24] report that force to remove 1–3-year-old *R. mangle* established in coarse coral rubble was greater than for those growing in sand or peat. The authors suggest this observation was likely due to burial of the seedling stems in coarse particles and not solely the result of rooting strength. Additionally, sample size of seedlings tested in [24] was small (N < 20 seedlings per treatment).

While effects of sediment texture were not detected in mangrove forests in this study, it must be understood that mangrove seedlings in the field were selected from areas of natural recruitment. Mangrove seedlings were not found established in areas characterized by coarse grain sizes, inherently suggesting selection away from this habitat feature. It is therefore possible that the effect of coarse sediment grain sizes to mangrove recruitment and retention is both present and deleterious. For instance, Kibler et al. [42] found a mean of four mangrove seedlings per transect meter established within a mature mangrove forest while no seedlings had recruited to a nearby shoreline where mangrove vegetation had been restored six years prior. As measured hydrodynamic conditions were similar in the restored and natural vegetation, the lack of sustained recruitment in the restored site was attributed to the legacy of erosion in the armored, coarse sediments of the restored shoreline. It has been reported that coarser sediments can potentially limit the successful establishment of mangroves by obstructing anchoring during early recruitment stages [64] and then may have a negative effect to mangrove biomass production [65]; however, these observations also could indirectly reflect hydrodynamic stress, which could be correlated with coarse sediments. Further investigation of coupled flow and sediment influence on mangrove recruitment and retention is warranted.

Root interactions between mangrove seedlings and surrounding vegetation significantly increased anchoring force for both species of mangrove tested in the forest. This finding provides quantitative evidence as to mechanisms that may hinder seedling retention along unvegetated shorelines and can be applied to enhance retention of seedlings that recruit into restored mangrove forests. It is known that established vegetation influences the local hydrodynamic environment [66], which can be of critical importance in areas where hydrodynamic forces may dislodge establishing seedlings [67]. For instance, previous studies have shown that salt-marsh vegetation can attenuate hydrodynamic stress along shorelines [68], including in the vicinity of restored mangrove vegetation [36], and encourage mangrove recruitment by trapping propagules (e.g., [69]). However, this is the first study to directly demonstrate the additional benefit of increased anchoring strength afforded by association with existing vegetation. In this study, mangrove-seedling roots interacted most frequently with pneumatophores of mature *A. germinans*. Whether the same anchoring effect would be found in association with species often selected as companion plantings with mangrove in restoration, for instance halophytic grasses (e.g., *Spartina alterniflora*) or herbaceous vegetation (e.g., *Batis maritima*), is a question that should be explored.

4.3. Mangrove Seedling Susceptibility to Instantaneous Hydrodynamic Removal

Based on anchoring force data collected from the field, it was estimated that the lowest velocities that could possibly dislodge *A. germinans* seedlings instantaneously was 1.50 m/s and *R. mangle* seedlings may become susceptible when velocities exceed 1.20 m/s. These minimum velocity thresholds are estimates based on measured force to remove seedlings recruited within 7 to 11 months from mangrove forest when the surrounding sediments around the seedlings are intact and not eroded. Thus, these are estimates associated with instantaneous seedling failure, Type I removal. The minimum critical uprooting velocities estimated based on measured anchoring force would be observed rarely in the study areas. For instance, hydrodynamic observations in Mosquito Lagoon during

typical conditions have measured channel velocities in the range of 0.2–0.4 m/s at peak tidal exchange, but flows within mangrove forest are an order of magnitude lower [42,70]. The comparison of measured velocity to estimated minimum critical velocities suggests that, after naturally recruited mangrove seedlings have been established for over several months, Type I uprooting is unlikely to be a dominant mechanism for removal. Reduction in anchoring force, for instance, through erosion of sediments either locally around the seedling roots (Type IIa) or by larger scale bed-degradation processes (Type IIb), must occur before seedlings would be removed by hydrodynamic force. This is similar to conclusions reached in studies of established river bar and bank vegetation [28,29] as well as newly germinated grain seedlings [60]. However, Type I uprooting of newly established mangrove seedlings with root lengths less than 4 cm was induced in a flume [23], suggesting that the removal mechanism may vary over mangrove seedling age. Further research is needed to better constrain application of Type I and II removal mechanisms as a function of mangrove seedling stage and estimate the levels of local or general erosion sufficient to reduce anchoring to the point of failure under varied hydrodynamic conditions.

5. Conclusions

Vegetation recruited to dynamic coastal environments may be subject to hydrodynamic dislodgment when drag forces surpass anchoring force. Despite potentially far-reaching implications to mangrove restoration and long-term sustainability of mangrove habitats, little is known about the hydrodynamic habitat thresholds that enable mangrove-seedling retention in natural forests. In this study, anchoring force of two species of mangrove (*R. mangle* and *A. germinans*) was measured in situ in mangrove forests and in laboratory-based experiments. Variation in seedling susceptibility to uprooting was quantified as a function of species, seedling age, morphometric variables and site characteristics to inform physical conditions and mechanisms that may lead to hydrodynamic seedling removal.

The anchoring force of *R. mangle* consistently exceeded *A. germinans*, reflecting the greater seedling biomass of the former. However, in both laboratory and field testing, force to remove *A. germinans* seedlings increased at a greater rate with growth (*A. germinans*: 0.20–0.23 N per g biomass; *R. mangle*: 0.04–0.07 N per g biomass), suggesting that the observed difference in species-specific anchoring force may eventually equalize or reverse. Anchoring force for both species was positively related to association with surrounding vegetation. Thresholds in mangrove seedling development related to anchoring force and failure mechanism were detected during early seedling establishment. Seedlings established for 1 month failed due to root pull out while older seedling failed via root breakage. The observed shift in failure mechanism indicates that anchoring force of newly established seedlings is limited by root size and architecture while older/larger seedlings are limited by root tensile strength. Expressing measured anchoring force as critical velocities that would remove seedlings tested in the field (minimum flows of 1.20–1.50 m/s) revealed that *A. germinans* and *R. mangle* seedlings become susceptible to spontaneous uprooting at velocities well above those measured in the study vicinity under typical conditions. This suggests that, after mangrove seedlings have sufficiently established, hydrodynamic removal is likely to be associated with a decline in anchoring force, for instance, through sequential erosion of sediments from around the plant base.

This study provides quantitative benchmarks in factors that may limit retention of naturally recruited or planted seedlings. Coastal environments are undergoing unprecedented changes driven by coastal development, sea level rise, and changing hydro-climatic drivers. Mangrove recruitment and conditions limiting success at early-life stages are pertinent to the design of successful natural infrastructure and mangrove-forest restoration, for instance, for applications of climate mitigation and adaptation projects within tropical and subtropical regions. Natural infrastructure such as rehabilitated mangrove forests will not be sustainable in the long term until they attain a level of propagule recruitment and seedling retention sufficient to maintain the forest structure.

Understanding factors affecting seedling establishment, especially those related to hydrodynamic and sediment dynamics, can inform design strategies that mitigate bottlenecks to long-term sustainable forest succession. For example, the quantitative hydrodynamic thresholds observed in this study indicate that seedling removal is likely to be associated with degradational processes ranging from the plant to reach scale. Based on this mechanistic understanding, integrating basic sediment-transport dynamics into the restoration design process may illuminate both potential challenges and pathways to success.

Appendix A

Table A1. AICc weights of top four models for laboratory pull tests predicting change in horizontal force to removal (Horiz..Force..N.) as a function of below-ground biomass (BG.Biomass), species (Sp.), age, and sediment treatment (sed).

#	Model	AICc	Δ AICc
1	log(Horiz..Force..N.) ~ BG.Biomass × Sp. + sed × Age	126.1	0
2	log(Horiz..Force..N.) ~ BG.Biomass × Sp. + sed + Age	129.6	3.5
3	log(Horiz..Force..N.) ~ BG.Biomass × Sp. + Age	132.5	6.4
4	log(Horiz..Force..N.) ~ BG.Biomass + Sp. + sed + Age	140.5	14.4

Table A2. AICc weights of top four models for field pull tests predicting change in horizontal force to removal (Horiz..Force..N.) as a function of above-ground biomass (AG.Biomass), species (Sp.), Park, percent cover of surrounding vegetation (Per.Veg), and percent canopy cover (Perc.Canopy).

#	Model	AICc	Δ AICc
1	log(Horiz..Force..N.) ~ AG.Biomass..g. × Sp. + Per.Veg	239.5	0
2	log(Horiz..Force..N.) ~ AG.Biomass..g. ×Sp.+ factor(Perc.Canopy) + Per.Veg	241.2	1.7
3	log(Horiz..Force..N.) ~ AG.Biomass..g. × Sp.+ Per.Veg + Park	241.5	2.0
4	log(Horiz..Force..N.) ~ AG.Biomass..g. ×Sp.	241.8	2.3

References

1. Alongi, D.M. *The Energetics of Mangrove Forests*; Springer: Berlin/Heidelberg, Germany, 2009; 216p.

2. Barbier, E.B.; Hacker, S.D.; Kennedy, C.; Koch, E.W.; Stier, A.C.; Silliman, B.R. The value of estuarine and coastal ecosystem services. *Ecol. Monogr.* **2011**, *81*, 169–193, doi:10.1890/10-1510.1.

3. Luther, D.A.; Greenberg, R. Mangroves: A Global Perspective on the Evolution and Conservation of Their Terrestrial Vertebrates. *BioScience* **2009**, *59*, 602–612, https://doi.org/10.1525/bio.2009.59.7.11.

4. Carugati, L.; Gatto, B.; Rastelli, E.; Martire, M.L.; Coral, C.; Greco, S.; Danovaro, R. Impact of mangrove forests degradation on biodiversity and ecosystem functioning. *Sci. Rep.* **2018**, *8*, 13298, https://doi.org/10.1038/s41598-018-31683-0.

5. McClenachan, G.M.; Donnelly, M.J.; Shaffer, M.N.; Sacks, P.E.; Walters, L.J. Does size matter? Quantifying the cumulative impact of small-scale living shoreline and oyster reef restoration projects on shoreline erosion. *Restor. Ecol.* **2020**, *28*, 1365–1371, https://doi.org/10.1111/rec.13235.

6. Tanaka, N.; Sasaki, Y.; Mowjood, M.I.M.; Jinadasa, K.B.S.N.; Homchuen, S. Coastal vegetation structures and their functions in tsunami protection: Experience of the recent Indian Ocean tsunami. *Landsc. Ecol. Eng.* **2007**, *3*, 33–45, https://doi.org/10.1007/s11355-006-0013-9.

7. Mazda, Y.; Wolanski, E.; King, B.; Sase, A.; Ohtsuka, D.; Magi, M. Drag force due to vegetation in mangrove swamps. *Mangroves Salt Marshes* **1997**, *1*, 193–199, https://doi.org/10.1023/a:1009949411068.

8. Cheong, S.-M.; Silliman, B.; Wong, P.P.; Van Wesenbeeck, B.; Kim, C.-K.; Guannel, G. Coastal adaptation with ecological engineering. *Nat. Clim. Change* **2013**, *3*, 787–791, https://doi.org/10.1038/nclimate1854.

9. Polidoro, B.A.; Carpenter, K.E.; Collins, L.; Duke, N.C.; Ellison, A.M.; Ellison, J.C.; Farnsworth, E.J.; Fernando, E.S.; Kathiresan, K.; Koedam, N.E.; et al. The Loss of Species: Mangrove Extinction Risk and Geographic Areas of Global Concern. *PLoS ONE* **2010**, *5*, e10095, https://doi.org/10.1371/journal.pone.0010095.

10. Giri, C.; Ochieng, E.; Tieszen, L.L.; Zhu, Z.; Singh, A.; Loveland, T.; Masek, J.; Duke, N. Status and distribution of mangrove forests of the world using earth observation satellite data. *Glob. Ecol. Biogeogr.* **2011**, *20*, 154–159, https://doi.org/10.1111/j.1466-8238.2010.00584.x.

11. Food and Agriculture Organization of the United Nations. *The World's Mangroves 1980–2005: A Thematic Study Prepared in the Framework of the Global Forest Resources Assessment 2005*; FAO: Rome, Italy, 2007.

12. Silva, R.; Martínez, M.; Van Tussenbroek, B.; Guzmán-Rodríguez, L.; Mendoza, E.; López-Portillo, J. A Framework to Manage Coastal Squeeze. *Sustainability* **2020**, *12*, 10610, https://doi.org/10.3390/su122410610.

13. Cano-Ortiz, A.; Musarella, C.M.; Fuentes, J.C.P.; Gomes, C.J.P.; Del Rio, S.; Canas, R.Q.; Cano, E. *Analysis of the Conservation of Central American Mangroves Using the Phytosociological Method*; Mangrove Ecosystem Ecology and Function; Intech Publisher: London, U.K., 2018: pp. 189-206.

14. Lewis, R.R. Ecological engineering for successful management and restoration of mangrove forests. *Ecol. Eng.* **2005**, *24*, 403–418.

15. Friess, D.A.; Krauss, K.W.; Horstman, E.; Balke, T.; Bouma, T.J.; Galli, D.; Webb, E. Are all intertidal wetlands naturally created equal? Bottlenecks, thresholds and knowledge gaps to mangrove and saltmarsh ecosystems. *Biol. Rev.* **2012**, *87*, 346–366, https://doi.org/10.1111/j.1469-185x.2011.00198.x.

16. Krauss, K.W.; Lovelock, C.E.; McKee, K.L.; López-Hoffman, L.; Ewe, S.M.; Sousa, W.P. Environmental drivers in mangrove establishment and early development: A review. *Aquat. Bot.* **2008**, *89*, 105–127, https://doi.org/10.1016/j.aquabot.2007.12.014.

17. Fillyaw, R.M.; Donnelly, M.J.; Litwak, J.W.; Rifenberg, J.L.; Walters, L.J. Strategies for Successful Mangrove Living Shoreline Stabilizations in Shallow Water Subtropical Estuaries. *Sustainability* **2021**, *13*, 11704, https://doi.org/10.3390/su132111704.

18. Kathiresan, K. How do mangrove forests induce sedimentation? *Rev. Biol. Trop.* **2003**, *51*, 355–360.

19. Mazda, Y.; Kobashi, D.; Okada, S. Tidal-Scale Hydrodynamics within Mangrove Swamps. *Wetl. Ecol. Manag.* **2005**, *13*, 647–655, https://doi.org/10.1007/s11273-005-0613-4.

20. Cannon, D.; Kibler, K.; Donnelly, M.; McClenachan, G.; Walters, L.; Roddenberry, A.; Phagan, J. Hydrodynamic habitat thresholds for mangrove vegetation on the shorelines of a microtidal estuarine lagoon. *Ecol. Eng.* **2020**, *158*, 106070, https://doi.org/10.1016/j.ecoleng.2020.106070.

21. Constance, A.; Haverkamp, P.J.; Bunbury, N.; Schaepman-Strub, G. Extent change of protected mangrove forest and its relation to wave power exposure on Aldabra Atoll. *Glob. Ecol. Conserv.* **2021**, *27*, e01564, https://doi.org/10.1016/j.gecco.2021.e01564.

22. Iii, R.R.L. Ecologically based goal setting in mangrove forest and tidal marsh restoration. *Ecol. Eng.* **2000**, *15*, 191–198, https://doi.org/10.1016/s0925-8574(00)00070-7.

23. Balke, T.; Bouma, T.J.; Horstman, E.M.; Webb, E.L.; Erftemeijer, P.L.A.; Herman, P.M.J. Windows of opportunity: Thresholds to mangrove seedling establishment on tidal flats. *Mar. Ecol. Prog. Ser.* **2011**, *440*, 1–9, https://doi.org/10.3354/meps09364.

24. Boizard, S.D.; Mitchell, S.J. Resistance of red mangrove (*Rhizophora mangle* L.) seedlings to deflection and extraction. *Trees* **2011**, *25*, 371–381, https://doi.org/10.1007/s00468-010-0512-z.

25. Lima, K.O.D.O.; Tognella, M.M.P.; Cunha, S.R.; de Andrade, H.A. Growth models of *Rhizophora mangle* L. seedlings in tropical southwestern Atlantic. *Estuar. Coast. Shelf Sci.* **2018**, *207*, 154–163, https://doi.org/10.1016/j.ecss.2018.03.021.

26. Minchinton, T.E. Canopy and substratum heterogeneity influence recruitment of the mangrove Avicennia marina. *J. Ecol.* **2001**, *89*, 888–902, https://doi.org/10.1046/j.0022-0477.2001.00599.x.

27. Edmaier, K.; Burlando, P.; Perona, P. Mechanisms of vegetation uprooting by flow in alluvial non-cohesive sediment. *Hydrol. Earth Syst. Sci.* **2011**, *15*, 1615–1627, https://doi.org/10.5194/hess-15-1615-2011.

28. Bywater-Reyes, S.; Wilcox, A.C.; Stella, J.C.; Lightbody, A.F. Flow and scour constraints on uprooting of pioneer woody seedlings. *Water Resour. Res.* **2015**, *51*, 9190–9206, https://doi.org/10.1002/2014wr016641.

29. Calvani, G.; Francalanci, S.; Solari, L. A Physical Model for the Uprooting of Flexible Vegetation on River Bars. *J. Geophys. Res. Earth Surf.* **2019**, *124*, 1018–1034, https://doi.org/10.1029/2018jf004747.

30. Le Minor, M.; Bartzke, G.; Zimmer, M.; Gillis, L.; Helfer, V.; Huhn, K. Numerical modelling of hydraulics and sediment dynamics around mangrove seedlings: Implications for mangrove establishment and reforestation. *Estuar. Coast. Shelf Sci.* **2019**, *217*, 81–95, https://doi.org/10.1016/j.ecss.2018.10.019.

31. Kamali, B.; Hashim, R. Mangrove restoration without planting. *Ecol. Eng.* **2011**, *37*, 387–391, https://doi.org/10.1016/j.ecoleng.2010.11.025.

32. Rabinowitz, D. Dispersal Properties of Mangrove Propagules. *Biotropica* **1978**, *10*, 47, https://doi.org/10.2307/2388105.

33. Friess, D.A.; Krauss, K.W.; Horstman, E.; Balke, T.; Bouma, T.J.; Galli, D.; Webb, E. Are all intertidal wetlands naturally created equal? Bottlenecks, thresholds and knowledge gaps to mangrove and saltmarsh ecosystems. *Biol. Rev.* **2012**, *87*, 346–366, https://doi.org/10.1111/j.1469-185x.2011.00198.x.

34. Cano, E.; Cano-Ortiz, A.; Veloz, A.; Alatorre, J.; Otero, R. Comparative analysis between the mangrove swamps of the Caribbean and those of the State of Guerrero (Mexico). *Plant Biosyst.-Int. J. Deal. all Asp. Plant Biol.* **2012**, *146*, 112–130, https://doi.org/10.1080/11263504.2012.704885.

35. Mckee, K.L. Interspecific Variation in Growth, Biomass Partitioning, and Defensive Characteristics of Neotropical Mangrove Seedlings—Response to Light and Nutrient Availability. *Am. J. Bot.* **1995**, *82*, 299–307, https://doi.org/10.1002/j.1537-2197.1995.tb12634.x.

36. López-Hoffman, L.; Ackerly, D.D.; Anten, N.P.R.; DeNoyer, J.L.; Martinez-Ramos, M. Gap-dependence in mangrove life-history strategies: A consideration of the entire life cycle and patch dynamics. *J. Ecol.* **2007**, *95*, 1222–1233, https://doi.org/10.1111/j.1365-2745.2007.01298.x.

37. Service, N.P. De Soto National Memorial. 2019. Available online: https://www.nps.gov/deso/index.htm (accessed on 23 May 2022).

38. Service, N.P. Canaveral National Seashore Florida. 2019. Available online: http://www.nps.gov/cana/index.htm (accessed on 23 May 2022).

39. Phlips, E.J.; Badylak, S.; Lasi, M.A.; Chamberlain, R.; Green, W.C.; Hall, L.M.; Hart, J.A.; Lockwood, J.C.; Miller, J.D.; Morris, L.J.; et al. From Red Tides to Green and Brown Tides: Bloom Dynamics in a Restricted Subtropical Lagoon Under Shifting Climatic Conditions. *Estuaries Coasts* **2015**, *38*, 886–904, https://doi.org/10.1007/s12237-014-9874-6.

40. McNulty, J.K.; Lindall, W.N.; Sykes, J.E. *Cooperative Gulf of Mexico estuarine inventory and study, Florida: Phase 1, Area Description*; US Department of Commerce, National Oceanographic and Atmospheric Association, Seattle, Washington: 1972; Volume 368, https://doi.org/10.5962/bhl.title.63164.

41. Caratti, J.F. Line intercept: Sampling Method. 2006. Available online: https://www.fs.fed.us/rm/pubs/rmrs_gtr164/rmrs_gtr164_11_line_inter.pdf (accessed on 23 May 2022).

42. Kibler, K.M.; Kitsikoudis, V.; Donnelly, M.; Spiering, D.W.; Walters, L. Flow–Vegetation Interaction in a Living Shoreline Restoration and Potential Effect to Mangrove Recruitment. *Sustainability* **2019**, *11*, 3215, https://doi.org/10.3390/su11113215.

43. Spiering, D.W.; Kibler, K.M.; Kitsikoudis, V.; Donnelly, M.J.; Walters, L.J. Detecting hydrodynamic changes after living shoreline restoration and through an extreme event using a Before-After-Control-Impact experiment. *Ecol. Eng.* **2021**, *169*, 106306, https://doi.org/10.1016/j.ecoleng.2021.106306.

44. Lightbody, A.F. and H.M. Nepf, Prediction of velocity profiles and longitudinal dispersion in emergent salt marsh vegetation. *Limnol. Oceanogr.* **2006**, *51*, 218–228.

45. Liu, C.; Evett, J. *Soil Properties, Testing, Measurement and Evaluation*; Prentice-Hall, Inc.: Hoboken, NJ, USA, 1997.

46. Bolker, B.; Bolker, M.B. Package 'bbmle'. Tools for General Maximum Likelihood Estimation, 2022. Available online: https://cran.r-project.org/web/packages/bbmle/bbmle.pdf (accessed on 23 May 2022)..

47. Team, R.C. *R: A Language and Environment for Statistical Computing*; R Foundation for Statistical Computing: Vienna, Austria, 2018.

48. Wickham, H. *ggplot2: Elegant Graphics for Data Analysis*; Springer: Berlin/Heidelberg, Germany, 2016.

49. Struve, J.; Falconer, R.; Wu, Y. Influence of model mangrove trees on the hydrodynamics in a flume. *Estuar. Coast. Shelf Sci.* **2003**, *58*, 163–171, https://doi.org/10.1016/s0272-7714(03)00072-6.

50. Mullarney, J.C.; Henderson, S.M. Flows Within Marine Vegetation Canopies. *Adv. Coast. Hydraul.* **2018**, 1–46, https://doi.org/10.1142/9789813231283_0001.

51. Coutts, M.P. Components of Tree Stability in Sitka Spruce on Peaty Gley Soil. *Forestry* **1986**, *59*, 173–197, https://doi.org/10.1093/forestry/59.2.173.

52. Moore, J.R. Differences in maximum resistive bending moments of Pinus radiata trees grown on a range of soil types. *For. Ecol. Manag.* **2000**, *135*, 63–71, https://doi.org/10.1016/s0378-1127(00)00298-x.

53. Peltola, H.; Kellomäki, S.; Hassinen, A.; Granander, M. Mechanical stability of Scots pine, Norway spruce and birch: An analysis of tree-pulling experiments in Finland. *For. Ecol. Manag.* **2000**, *135*, 143–153, https://doi.org/10.1016/s0378-1127(00)00306-6.

54. Nicoll, B.C.; Gardiner, B.A.; Rayner, B.; Peace, A.J. Anchorage of coniferous trees in relation to species, soil type, and rooting depth. *Can. J. For. Res. -Rev. Can. Rech. For.* **2006**, *36*, 1871–1883.

55. Burylo, M.; Rey, F.; Roumet, C.; Buisson, E.; Dutoit, T. Linking plant morphological traits to uprooting resistance in eroded marly lands (Southern Alps, France). *Plant Soil* **2009**, *324*, 31–42, https://doi.org/10.1007/s11104-009-9920-5.

56. Bankhead, N.L.; Thomas, R.E.; Simon, A. A combined field, laboratory and numerical study of the forces applied to, and the potential for removal of, bar top vegetation in a braided river. *Earth Surf. Process. Landf.* **2017**, *42*, 439–459, https://doi.org/10.1002/esp.3997.

57. Karrenberg, S.; Blaser, S.; Kollmann, J.; Speck, T.; Edwards, P.J. Root anchorage of saplings and cuttings of woody pioneer species in a riparian environment. *Funct. Ecol.* **2003**, *17*, 170–177, https://doi.org/10.1046/j.1365-2435.2003.00709.x.

58. Liu, Y. The root anchorage ability of Salix alba var. tristis using a pull-out test. *Afr. J. Biotechnol.* **2011**, *10*, https://doi.org/10.5897/ajb10.1499.

59. Schutten, J.; Dainty, J.; Davy, A.J. Root anchorage and its significance for submerged plants in shallow lakes. *J. Ecol.* **2005**, *93*, 556–571, https://doi.org/10.1111/j.1365-2745.2005.00980.x.

60. Edmaier, K.; Crouzy, B.; Ennos, R.; Burlando, P.; Perona, P. Influence of root characteristics and soil variables on the uprooting mechanics of *Avena sativa* and Medicago sativa seedlings. *Earth Surf. Process. Landforms* **2014**, *39*, 1354–1364, https://doi.org/10.1002/esp.3587.

61. Poorter, H.; Nagel, O. The role of biomass allocation in the growth response of plants to different levels of light, CO2, nutrients and water: A quantitative review. *Funct. Plant Biol.* **2000**, *27*, 1191–1191, https://doi.org/10.1071/pp99173_co.

62. Simpson, L.; Osborne, T.; Feller, I. Establishment and Biomass Allocation of Black and Red Mangroves: Response to Propagule Flotation Duration and Seedling Light Availability. *J. Coast. Res.* **2017**, *335*, 1126–1134, https://doi.org/10.2112/JCOASTRES-D-16-00108.1.

63. Oplatka, M.; Sutherland, A. Tests on willow poles used for river bank protection. *J. Hydrol.* **1995**, *33*, 35–58.

64. Donnelly, M.; Shaffer, M.; Connor, S.; Sacks, P.; Walters, L. Using mangroves to stabilize coastal historic sites: Deployment success versus natural recruitment. *Hydrobiologia* **2017**, *803*, 389–401, https://doi.org/10.1007/s10750-017-3155-x.

65. Duarte, C.; Geertz-Hansen, O.; Thampanya, U.; Terrados, J.; Fortes; Kamp-Nielsen, L.; Borum, J.; Boromthanarath, S. Relationship between sediment conditions and mangrove Rhizophora apiculata seedling growth and nutrient status. *Mar. Ecol. Prog. Ser.* **1998**, *175*, 277–283, https://doi.org/10.3354/meps175277.

66. Norris, B.K.; Mullarney, J.C.; Bryan, K.R.; Henderson, S.M. Turbulence Within Natural Mangrove Pneumatophore Canopies. *J. Geophys. Res. Oceans* **2019**, *124*, 2263–2288, https://doi.org/10.1029/2018jc014562.

67. Thampanya, U.; Vermaat, J.; Duarte, C.M. Colonization success of common Thai mangrove species as a function of shelter from water movement. *Mar. Ecol. Prog. Ser.* **2002**, *237*, 111–120, https://doi.org/10.3354/meps237111.

68. Bouma, T.J.; Vries, M.B.D.; Low, E.; Kusters, L.; Herman, P.M.J.; Tanczos, I.C.; Temmerman, S.; Hesselink, A.; Meire, P.; Regenmortel, S.V. Flow hydrodynamics on a mudflat and in salt marsh vegetation: Identifying general relationships for habitat characterisations. *Hydrobiologia* **2005**, *540*, 259–274, https://doi.org/10.1007/s10750-004-7149-0.

69. Stevens, P.W.; Fox, S.L.; Montague, C.L. The interplay between mangroves and saltmarshes at the transition between temperate and subtropical climate in Florida. *Wetl. Ecol. Manag.* **2006**, *14*, 435–444, https://doi.org/10.1007/s11273-006-0006-3.

70. Cannon, D.; Kibler, K.; Walters, L.; Chambers, L. Hydrodynamic and biogeochemical evolution of a restored intertidal oyster (*Crassostrea virginica*) reef. *Sci. Total Environ.* **2022**, *831*, 154879. https://doi.org/10.1016/j.scitotenv.2022.154879.